Received: 01 June 2022 | Revised: 24 June 2022 | Accepted: 01 July 2022
DOI: 10.22034/ecc.2022.345188.1484
Eurasian Chemical Communications
SAMI

FULL PAPER

Synthesis, characterization, and *in vitro* study of novel modified reduced graphene oxide (RGO) containing heterocyclic compounds as anti-breast cancer

Hussein Ali Fadhil[a,*] |Ali H. Samir[a] |Yusra Abdulghafoor Mohammed[b] |Zeinab M.M. Al Rubaei[a]

[a]*Department of Chemistry, College of Education for Pure Science Ibn Al–Haitham, University of Baghdad, Adhamiyah, Anter square, Baghdad, Iraq*

[b]*Techniques Department, Al- Yarmouk College-Medical Laboratory, University of Al- Yarmouk, Diyala, Iraq*

Nano derivatives of graphene sheets were prepared by functionalized with triazoles. Starting with thiocarbohyderazide which was obtained by refluxing a combination of carbon disulfide and hydrazine hydrate (I), it generated 3-thiol-4-amino-1,2,4-triazole when heated in solid state(II). Anthranilic acid was reacted with (C6H5COCl) to produce 2-phenyl-4H-benzo[d][1,3]oxazin-4-one(III), which was then condensed with the 3-thiol-4-amino-1,2,4-triazol(II) in glacial acetic acid to produce (IV) compound. In addition, the (h2, h3, h4) compounds were used to exfoliate graphite (h1) which contains graphite rods as both anode and cathode, electrolyte, distilled water, sodium bicarbonate, and a power source for the formation of graphene oxide, graphite oxides with a variables acid (h2). Graphene oxide's interaction with hydrazinehydrate yielded (RGO) (h3). The product of (RGO) sonification with thionyl chloride in DMF yielded acyl chloride-functionalized reduced graphene oxide (RGO-COCl) (h4). Compound (IV) was created by reacting (RGO-CO-Cl) with dry THF and Et3N to yield compound (RGO-CO-Cl) (V). Concerning physical features and spectral properties, validity of compounds established by FTIR spectroscopy, and some of them by 1H, 13C-NMR spectrum, XRD, SEM, and AFM. The MCF-7 and VRL-68 cell lines were used to investigate anti-breast cancer and anti-hepatic cancer activity, which could be used as a foundation for the development of novel anticancer medicines.

***Corresponding Author:**
Hussein Ali Fadhil
Email: hassensat06@gmail.com
Tel.:+967711320987

KEYWORDS

Anti-breast cancer; nanographene oxide functionalization; quinazoline; triazole.

Introduction

Because of their unusual physiochemical properties, graphene and GO based nanomaterials have piqued researchers' curiosity. It can be used in a variety of biological domains due to its 2D allotropic nature. Graphene and its composites have biomedical applications such as gene and tiny molecule medicine delivery. It is also utilized to biofunctionalize proteins, as an anticancer drug, and as an antibacterial bone and teeth implantation agent. The newly synthesized nanomaterials' biocompatibility permits them to be used extensively in medicine and biology [1].

Over the last decade, nanomaterials have been a major study topic for cancer

treatment. Nanomaterial's, polymeric nanomaterials, metal nanoparticles, semiconductor quantum dots, and carbon-based nanomaterials such as (GO) have been used for cancer cell imaging, chemotherapeutic drug targeting, chemotherapy, photothermal therapy, and photodynamic employed therapy [2].

In the field of medication delivery, graphene oxide has piqued interest. Nano scale graphene oxide (NGO) was commonly used to load anti-cancer medications due to its sp2-aromatic structure and abundance of oxygen-containing groups, resulting in great loading efficiency [3].

Graphene is a versatile carbon nanomaterial that has the potential to be used in cancer therapeutic platform technologies. Anticancer drugs and functional groups that target cancer cells and tissue can be covalently and non-covalently functionalized on its surface to improve therapeutic efficacies. Its physicochemical properties can also be exploited to simplify the delivery of stimulus-responsive therapies and medications [4, 5].

The technology for functionalizing graphene and making it suitable for biological applications has been devised. Graphene oxide nanoplatelets is used to destroy malignant cells by artificially loading them with antibodies and to create images of living cells with a near-infrared (NIR) backdrop. NGO generated by altering Hummer's approach can be helpful. It can be manufactured in a scalable manner as a multifunctional biocompatible NGO with varying physical sizes for biological and medicinal purposes. Anticancer medications can be loaded onto it and transported to the patient's cancer cells [6].

The two general methods for organic covalent functionalization reactions of graphene are (a) the formation of covalent bonds between free radicals or dienophiles and C = C bonds of pristine graphene, and (b) the formation of covalent bonds between organic functional groups and the oxygen groups of GO. [7].

There appears to be about 8 million fatalities worldwide, with cancer being the second biggest cause of death [1]. Chemotherapy is still one of the most prevalent cancer treatment options. Small compounds have a low aqueous solubility; fast metabolism, removal of medications, failure to achieve the required target site non-specific cytotoxicity, multi-drug resistance, and concentration are all drawbacks of traditional drug delivery systems and treatment procedures. In recent years, the use of nanomaterials in cancer therapy has resulted in some cutting-edge research to address the aforementioned limits [8–10].

Graphene is utilized to find cancer cells in their earliest stages. The tumor sphere assay can be used to assess the functioning as well as the anchorage-independent clonal growth of an individual cancer stem cell. GO significantly inhibits the production of tumor spheres in a variety of cell lines, including ovarian, pancreatic, breast, lung, and glioblastoma malignancies. The fact that GO harms cancer cells less than normal fibroblastic cells is astounding [11].

Experimental

Materials

All the chemicals and solvents were purchased of A.R. Grade quality obtained from (Aldrich and BDH) were used without further purifications. On a SHIMADZU FTIR-8400S Fourier transform infrared spectra (400-4000 cm^{-1}) in KBr disk were recorded. Stunrt, UK, was used to determine the melting point. On a Fourier transformation Burker spectrometer operating at (400MHZ), ^{1}H,^{13}C-NMR was recorded (DMSO-d6), X-ray diffraction, Scanning Electron Microscopy, and Atomic Force Microscopy. The measurements were taken at Esfahan University's Department of Chemistry.

Preparation of nano materials

Preparation of exfoliated nano graphite from carbon rods (h1)

The electrochemical setup for exfoliating graphite usually includes the following components: Anode and cathode made of graphite rod [12], electrolyte is a type of electrolyte that is (1000 mL distilled water and 10 g sodium bicarbonate) with a 15V power supply for 24 hours, yielding 0.5 g graphite [13].

Preparation of graphene oxide (GO) (h2)

The procedure of Hummer was utilized [14]. For the synthesis of GO, oxidize the graphite as follows:

In an ice bath with a 500 mL reaction flask, 1 gm graphite, 1.5 gm $NaNO_3$, and 46 mL H_2SO_4 were combined and vigorously agitated at 0 ℃ for 15 minutes. Then, 6 gm $KMnO_4$ was slowly added to the aforementioned solution and allowed to cool for 30 minutes. Following that, the suspended solution was constantly agitated for 2 hours. Water (46 mL) was gently added to the suspension at 35 ℃ for 10 minutes, raising the temperature to 98 ℃. For the next 20 minutes, the solution was stirred. The suspension was then diluted with 140 mL warm water and stirred for 10 minutes. The solution was then kept at room temperature while being treated with 15 mL (30%) H_2O_2 to be converted left over Mg^{+2}soluble into permanganate. Finally, centrifugation was used to filter the suspension, which was then washed with 10 percent HCL and distilled water [15] and was dried in a vacuum oven at a temperature of 70 ℃ for 24 hours to acquire GO, as shown in Scheme 1.

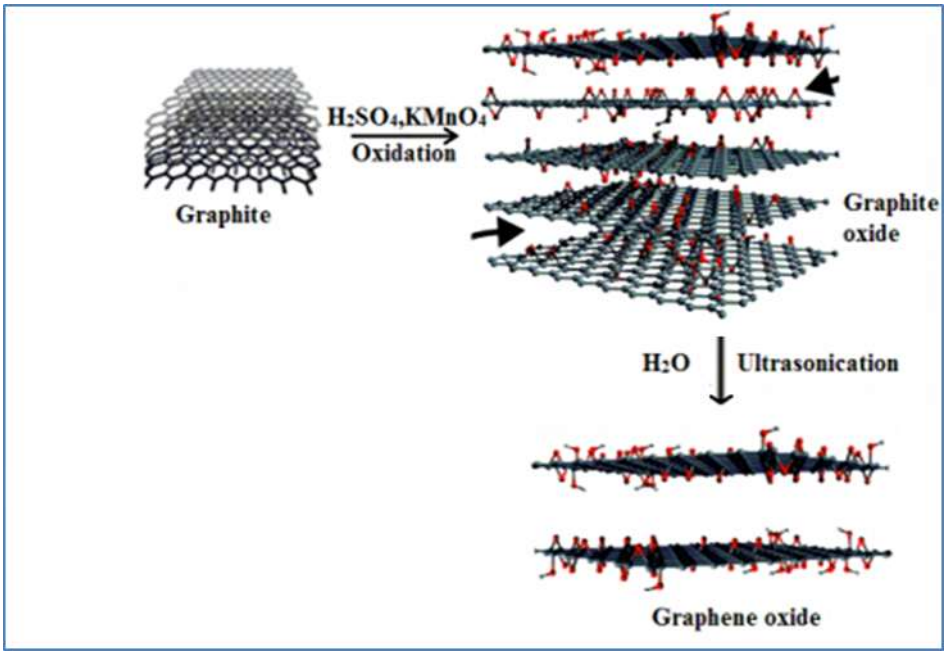

SCHEME 1 Oxidation of graphite to graphene oxide

Preparation of Reduced Graphene Oxide (RGO) by Hydrazine (h3)

100 mg graphene oxide was distributed in 1 mL HCl solution. After that, 1 mL of hydrazine monohydrate (80%) was added; the mixture was heated for 2 hours at 95 ℃. Then, RGO was collected through filtration [16]. The resulting product was washed with water many times to eliminate excess hydrazine before being dried in a vacuum oven at 100 ℃ for 12 hours, as indicated in Scheme 2.

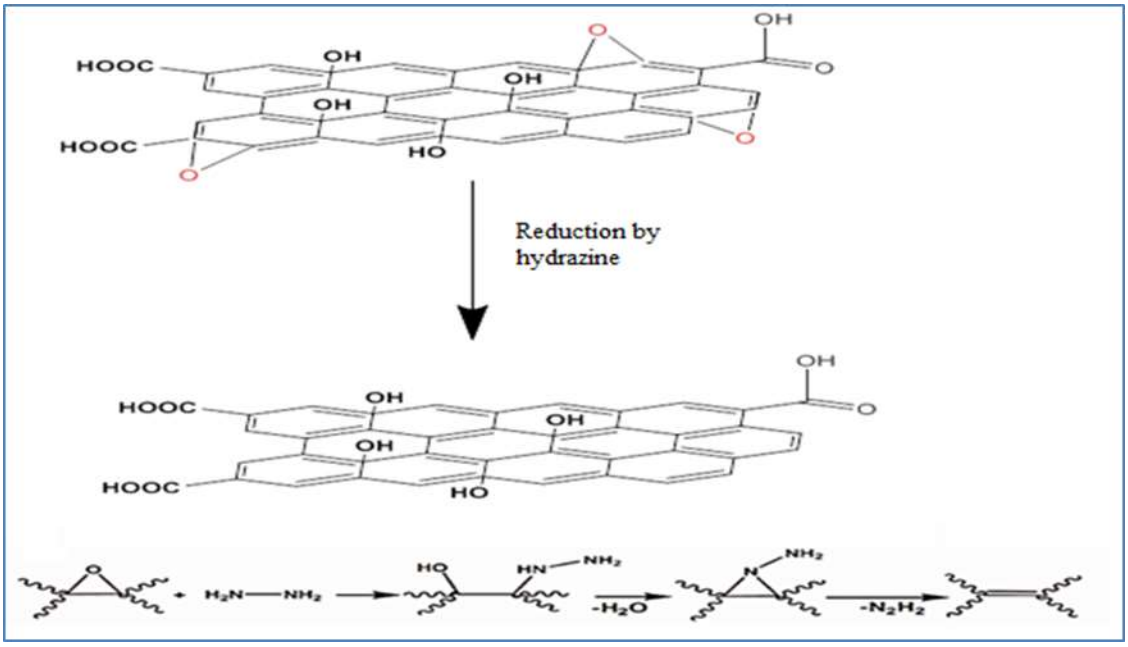

SCHEME 2 Reduced graphene oxide to RGO

Preparation of acylchloride-functionalized reduced graphene oxide RGO-COCl) (h4)

By sonification for 1 hour, graphene (0.1 g) was thoroughly dispersed in (10 mL) of dry (DMF), and then it was treated with $SOCl_2$ (60 mL, 0.82 mol) at 80 ℃ for 24 hours, 1, Centrifugation was used to separate the product, which was then washed with anhydrous THF and dried, as indicated in Equation 1 [17].

EQUATION 1 Preparation of acylchloride of RGO

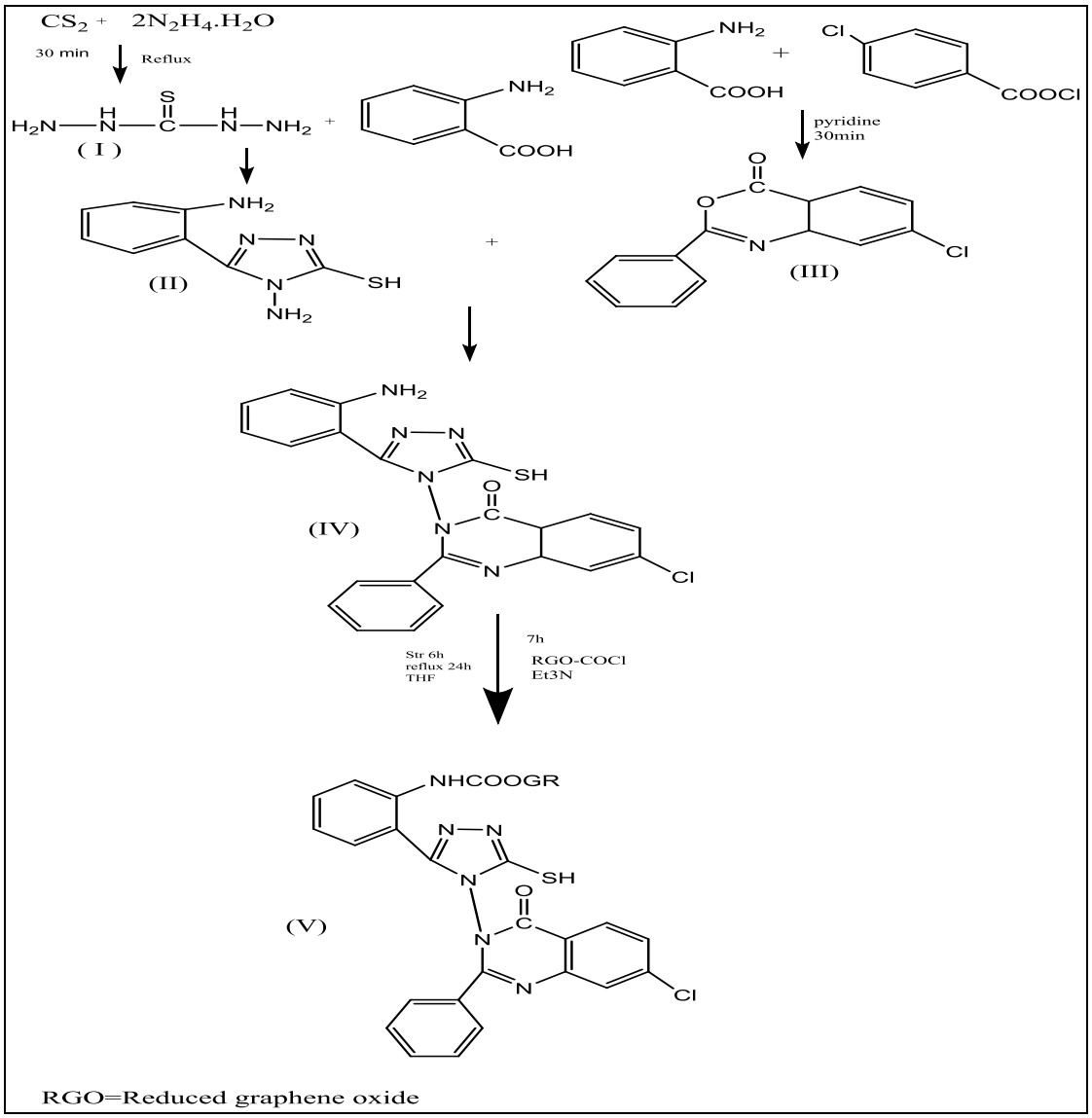

SCHEME 3

Preparation of thiocarbohydrazide (TCH) (I)

In an ice bath, in a (100 mL) round bottom flask (20 mL), carbon disulfide (CS_2) (5 mL) was added dropwise with stirring, and hydrazine hydrate was added drop by drop, stirring constantly. For 30 minutes, the mixture was refluxed until a yellow-white precipitate formed. Filtered and rinsed in ethanol, the yellow-white precipitate was recrystallized from water, and white crystals were produced, dried it in 70 °C for 4 hours, as indicated in Scheme 3 at melting point of (172-174) [18].

Preparation of 4-amino-5-(2-aminophenyl)-4H-1,2,4-triazole-3-thiol (II)

Placed in an around-bottom flask, a combination of 2-aminobenzoic acid (0.01 mol) and thiocarbohydrazide (TCH) (0.02 mol) was heated until melted. The product was treated with sodium bicarbonate solution after cooling. After that, the product was rinsed with water and filtered. A combination of dimethylformamide and ethanol was used to recrystallize the solid product, as indicated in Scheme 3, m.p (236-238) [19].

Preparation of 7-chloro-2-phenyl-4a,8a-dihydro-4H-benzo[d][1,3]oxazin-4-one (III)

To 4-chlorobenzoyl chloride, a solution of 2-aminobenzoic acid (Anthranilic acid) (0.01 mol) in (30 mL) pyridine was added (0.02 mol). The mixture was shaken for 5 minutes before being set aside at room temperature for another 25 minutes, shaking occasionally. The crude product was recrystallized from absolute ethanol after being treated with 10% $NaHCO_3$ (15 mL), filtered, washed with water, and dried, as indicated in Scheme 3, m.p (145-147) [20].

Preparation of 3-(3-(2-aminophenyl)-5-mercapto-4H-1,2,4-triazol-4-yl)-7-chloro-2-phenyl-4a,8a-dihydroquinazolin-4(3H)-one (IV)

A mixture of equilmolar quantities (0.001 mol) of 7-chloro-2-phenyl-4a, 8a-dihydro-4H-benzo[d][1,3]oxazin-4-one (III) was provided with (4-amino-1,2,4-triazol(II) presence of (15 mL) of Gla.CH_3COOH. Refluxing the mixture was done for 5 hours. Then, with (25 mL) of ice cold distilled water was added to the reaction media, the chemicals were filtered, dried, and recrystallized from ethanol, as indicated in Scheme 3, m.p (230-232) [21].

Preparation of reduced graphene oxide-triazol amide (V)

The reaction between RGO-COCl and compound (IV) led to the formation of grafted RGO to a dispersion of (RGO-COCl) (0.05 g) in (30mL) dry THF, in a nutshell, previously dried (IV) in (2 mL) at 0 °C, Tetrahydrofuran and Et_3N (1mL) were added dropwise. The mixture was mixed at room temperature for 1 hour, and then refluxed for 24 hours at 0 °C. as indicated in Scheme 3. The powder was cleaned with deionized water and ethanol in excess. The resulting powder was washed and dried [22].

Biological analysis

The MTT (3-(4,5-dimethylthiazol-2-yl)-2,5-diphenyl tetrazolium bromide

Investigation was carried out according to the procedure indicated in the literature [23,24].

MTT assay

The MTT investigation would be estimation tool for the cytotoxicity synthetic materials compound (V) against MCF-7 (human, breast tumor, and one line of normal cells WRL-68 (Hepatic cell line from a human normal cell lines. The work was applied in Malaya University-College of Medicine-Pharmacology Department. Dimethyl-sulfoxide (DMSO) was added to the synthesized compound, to make a stock solution and dilutions in a series (6.25- 400 µg/mL). 100 µL of samples were added to MCF-7 and WRL-68 cell lines, and for 24 hours, the cell culture was incubated in a CO_2 incubator at 37 °C. 20 mL of MTT stock solution (6 µg/ mL) was added to each well and plates followed, and then were incubated for 1-4 hours. When the media was taken away, DMSO was already introduced per each well to dissolve the crystals of the formazan. The absorption rate was validated at 575 nm by employing a Hidex-Chameleonmicroplate reader (Sheffield, U.K. Lab Logic Systems). As a percentage of cell survival, the small portion of the absorbance of the treated cells with the produced compounds compared to the absorbance of untreated cells was computed. The IC50 compound values were calculated [25,26].

Statistical analysis

The computed data was analyzed using a one-way analysis of variances, whether the differences between the groups were statistically significant; the mean ± standard deviation of the data was determined. (Graph Pad program) Graph Pad Prism V6 was used to analyze the results statistical significance.

Results and discussion

Compound (I):thiocarbohydrazide (TCH)

However, the most popular way to make TCH is to combine CS_2 and hydrazine. To begin, CS_2 combines with hydrazine to make hydraziniumdithiocarbazinate (HDTC), a water-soluble salt that forms in approximately quantitative yield at low temperatures [27].The FT-IR spectrum data of compound (I) showed peaks at 3304, 3269, and 3165cm^{-1} corresponds to N-H and NH_2 stretching vibrations, respectively. The NH_2 bending and wagging vibrations contributed to the two peaks at 1637 and 1139 cm^{-1}, respectively. The characteristic peaks 1531 and 1490 cm^{-1} assigns to the coupled modes N-H wagging and C-N stretching vibrations, the C=S stretching contributes to two peaks at 1284 cm^{-1} and 927 cm^{-1}, respectively. Other vibrations, such as C-N stretching and C-N-N bending, are also present in these peaks.

Compound (II): 4-amino-5-(2-aminophenyl)-4H-1,2,4-triazole-3-thiol

The FT-IR spectrum data of compound [II], showed stretching vibration of *ν* (NH_2) aliphatic in (3522 and 3367.71) cm^{-1} and *ν* (NH_2) aromatic in (3400 and 3263.1), while ν (NH) was interested. The peak in (1666.5) assigns to the ν(C=N). The C=S stretching contributes to peak at 1149.58 cm^{-1}, also the peak at 1072.5 cm^{-1}corresponds to ν (N-N) [28].

Compound (III): 7-chloro-2-phenyl-4a,8a-dihydro-4H-benzo[d][1,3]oxazin-4-one [III]

The synthesized compound was characterized by FTIR and ^{1}H-NMR Spectroscopy. FT-IR spectrum of compound (III), displayed the appearance of band at (1765) cm^{-1} attributed to the (C=O) of cyclic ester, (1656) cm^{-1} due to the azomethine group and (1586) cm^{-1} due to the (C=C) bond. ^{1}H-NMR (DMSO)compound's spectrum (III). Figure 1 displays the next [29] chemical alterations that are recognizable, (DMSO-d6) ppm. At 6.41-8.64 ppm, the aromatic ring protons were appeared as numerous.

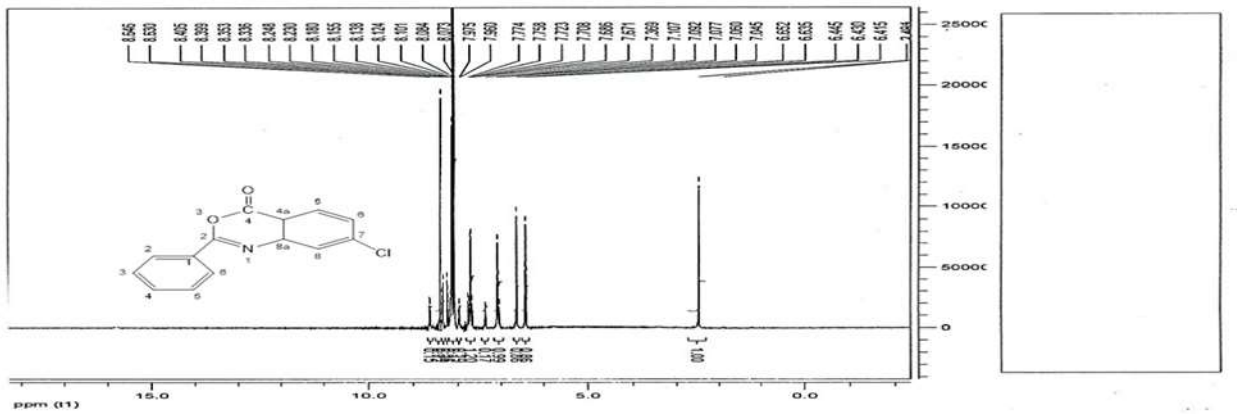

FIGURE 1 ^{1}H-NMR spectrum of compound [III]

Compound (IV): 3-(3-(2-aminophenyl)-5-mercapto-4H-1,2,4-triazol-4-yl)-7-chloro-2-phenyl-4a,8a-dihydroquinazolin-4(3H)-one [IV]

The FT-IR spectrum data of compound (IV), showed stretching vibration (NH_2) aliphatic in (3614 and 3525) cm^{-1}, and disappearance stretching vibration of (NH_2) aromatic in (3400, 3263) cm^{-1} of compound (II).The peak in (3100) cm^{-1} assigns to the *ν* (C-H) aromatic, the (C=O) of amide group observed at *ν* (1685) cm^{-1}, also the peak at (1523) cm^{-1} assigns to the ν(C=C) of aromatic ring. The ^{1}H-NMR (DMSO) spectrum data of compound

(IV), Figure 2, indicated the following signals: a triplet single at δ (1.18, 2.45) ppm for aliphatic saturated protons [30], singlet signal at δ (7.19) ppm for tautomerism of (NH) group, multiples signals at δ (7.20-8.65) ppm due to olefin and aromatic protons, and a singlet signal at δ (14.35) ppm for (SH) proton [31].^{13}C-NMR spectrum of compound (IV), Figure 3 showed signals of amide (C=O) carbonyl carbon at δ (170) ppm, ethylene (-CH=C-), (-C=N-), and aromatic carbons at δ (117-141) ppm, as well as (C=S) carbon at (164) ppm.

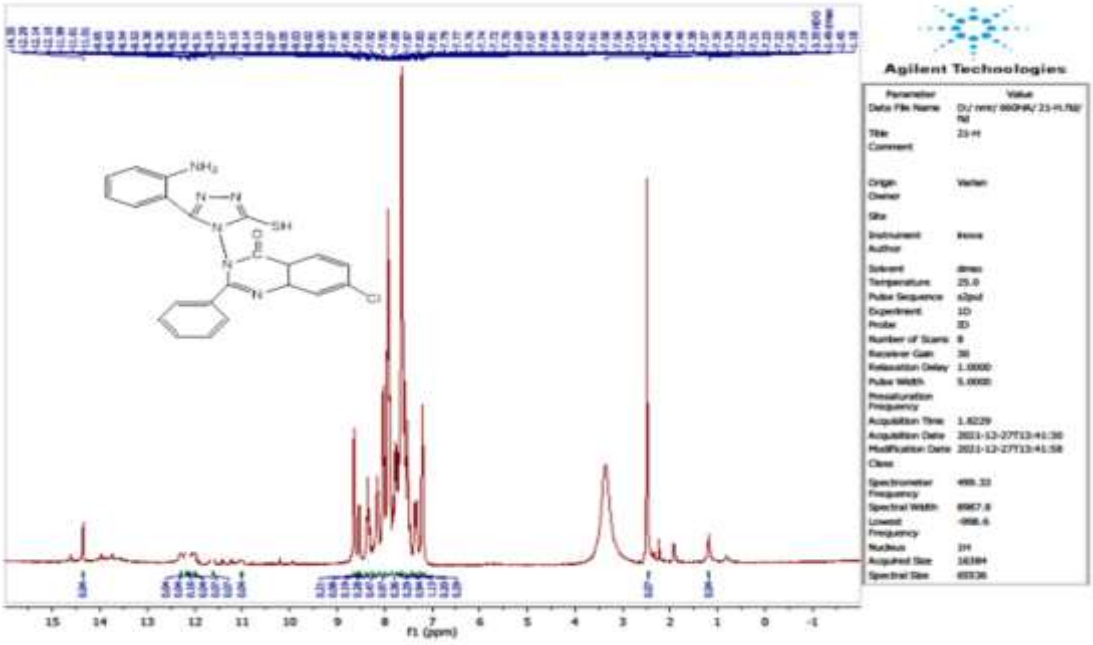

FIGURE 2 ^{1}H-NMR spectrum of compound [IV]

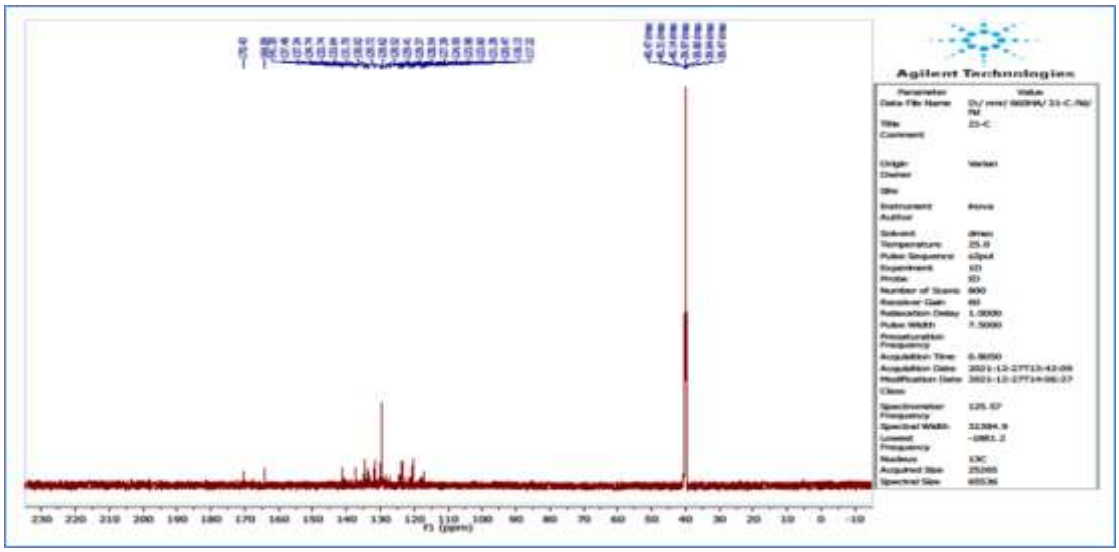

FIGURE 3 ^{13}c-NMR spectrum of compound [IV]

Compound (V): reduced graphene oxide-triazol amide RGO-AMIDE (V)

The infrared spectrum data of compound (V), revealed the following signals: a large peak at (3383) cm^{-1}, this peak is related to the stretching of *ν*(OH) group for RGO and appearance of absorption band at (1705) cm^{-1} due to C=O of carboxyl group. The C=O group of $RCONH_2$ noticed at (1662) cm^{-1}. The XRD

spectrum of graghene oxide in Figure 4 showed angle value at 2 theta (10.7 and 7.6) with the d-spacing between the layers (d=0.76) nm, and this indicates very good peeling which refers to the carbonyl, hydroxyl, carboxyl, and epoxy groups. As noted that law granule size (D=7.4) nm refer to a good repelled and good oxidation by hummer's method, because the numbers of layers in the sample (n=10).

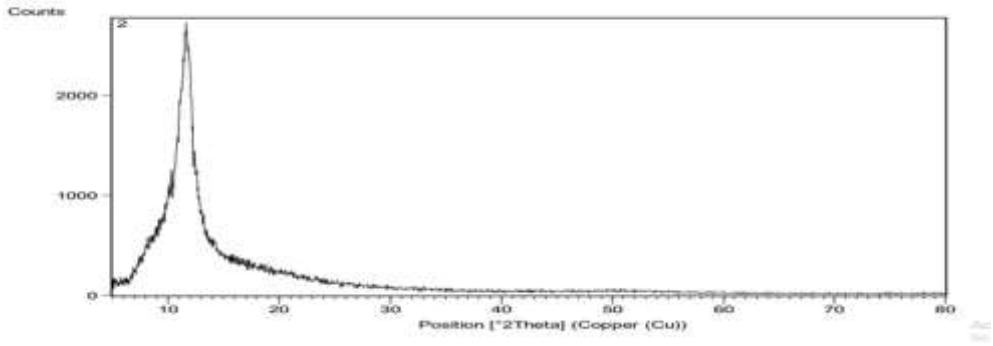

FIGURE 4 XRD patterns of RGO

From the morphological image FESEM of the GO compound, Figure 5 it was evident that there is a good roughness, as shown in the image (a) and this leads to an expected increase in the surface area as shown in the image (b), with a clear thickening on the page edges in the image (c) and spread folds on the surfaces in the plates in the image (d).

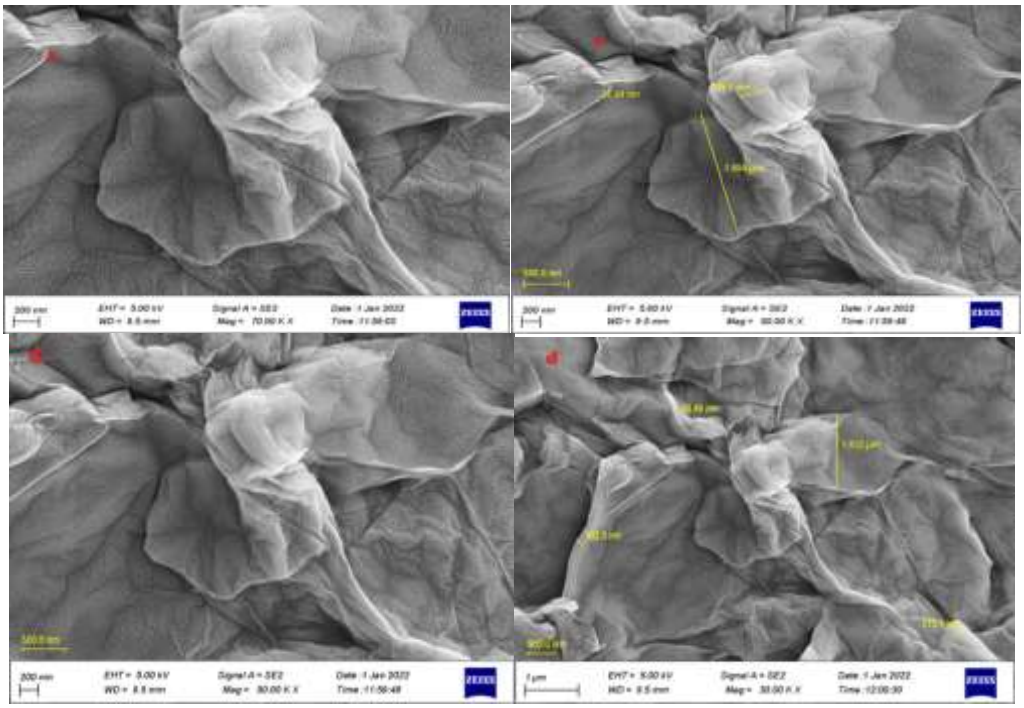

FIGURE 5 FESEM images of GO compound

Atomic force microscope (AFM) was also used to examine the morphology and the thickness of the RGO- sheets the morphology of the RGO was pictured and measured using AFM in Figure 6, that depicted the presence of gatherings on the surface with maximum height for roughness at (22) nm, and that was supported by optional curve 500 nm for the measured sample 1000*1000 nm.

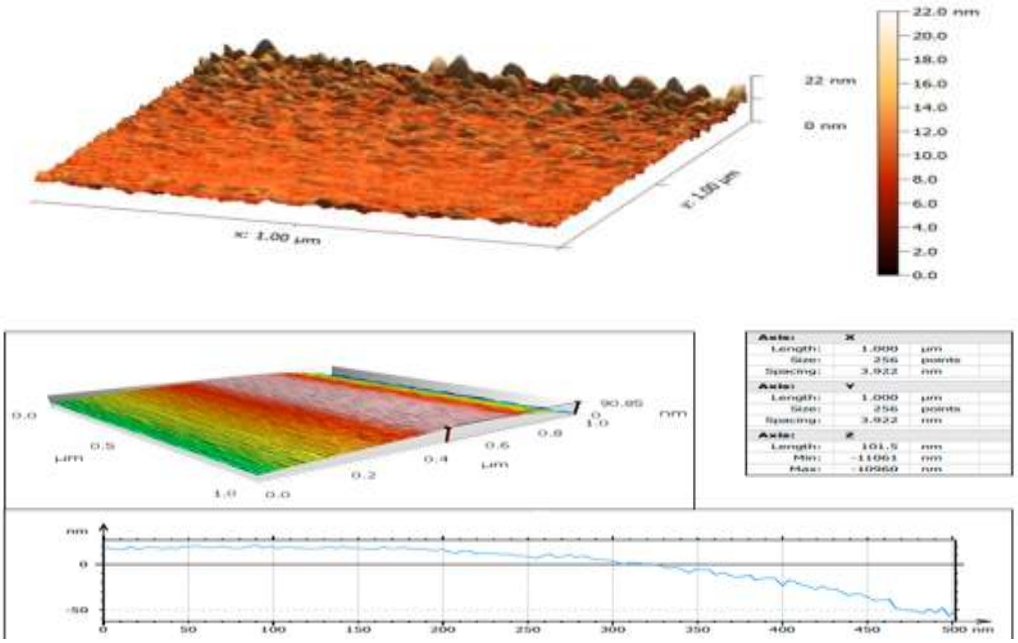

FIGURE 6 AFM image of RGO compound

In Figure 7, the XRD spectrum of reduced graphene oxide (RGO) indicated an angle value **2 θ (26.5)** with the d-spacing between the layers (d=0.33) and granule size D=43.8 nm as the number of layers grows at n=123.

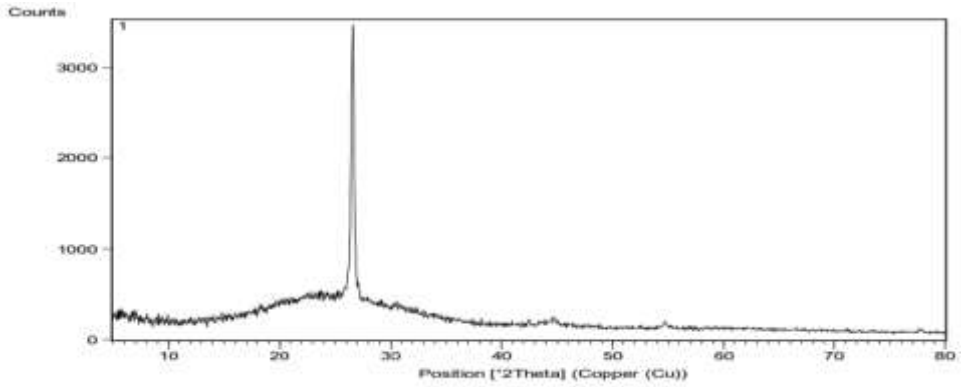

FIGURE 7 XRD patterns of RGO compound

From the morphological image FESEM of the GO compound, Figure 8, a good roughness was observed in the image (a) and this leads to an expected increase in the surface area, as depicted in images (E, F, G, and H).

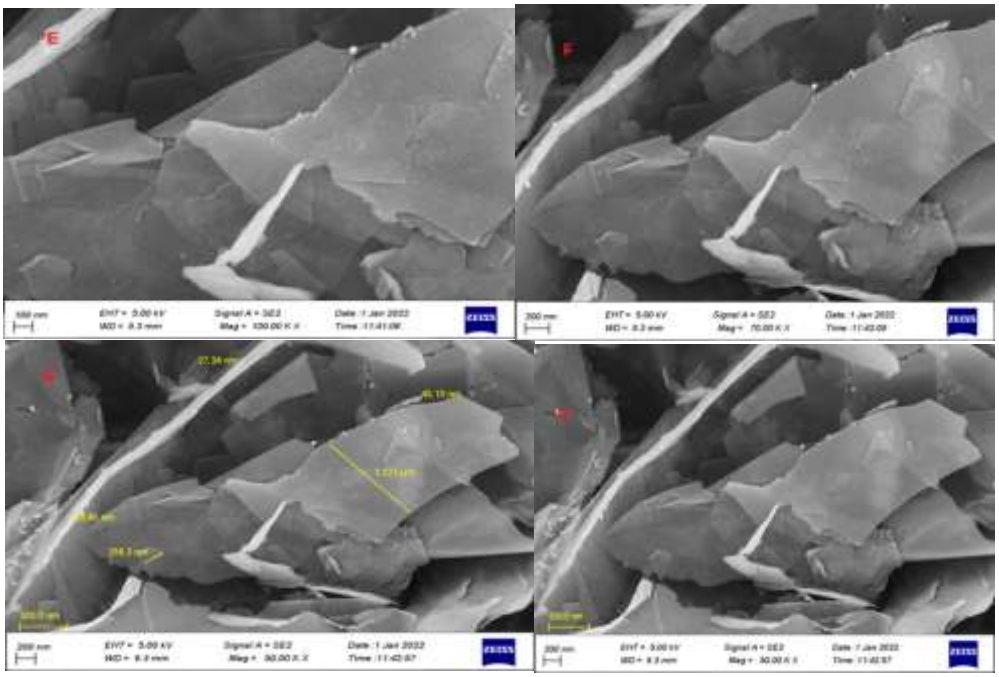

FIGURE 8 FESEM images of GO compound

As for the atomic force microscope (AFM) of the compound RGO, Figure 9, displays the presence of gatherings on the surface with maximum height for the roughness at (6.1) nm, and that was support by optional curve 500 nm for the measured sample at 1000*1000 nm.

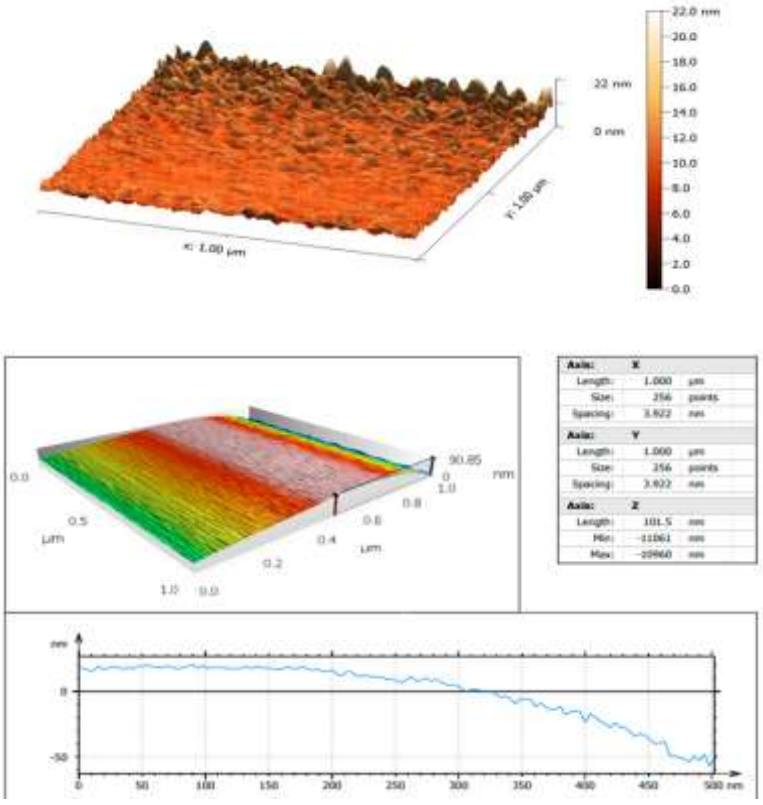

FIGURE 9 AFM image of RGO compound

In Figure 10, from the comparison between the granule size, (D=48.7) and d-spacing between layers (d=10), and also the numbers of the sheets in the layers (n=4.8), we noticed a change in the crystaline shape with increased granule size and the number of layers, this is logical with adding compound (V).

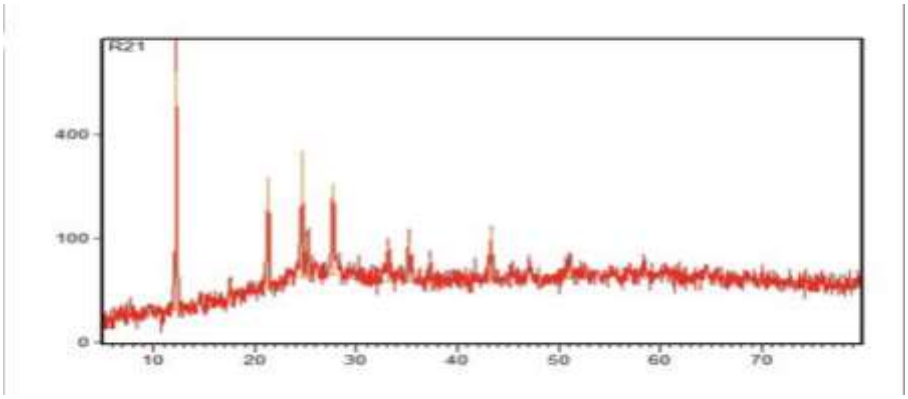

FIGURE 10 XRD patterns of compound (V)

Figure 11 shows the SEM image of compound (V). From noticing the morphological image of this compound, we notice that there is irregular fracture an average (31.3) nm image (a) and the presence of randomly distributed accumulation of compound (V) in the middle of the sheets in the form of separate granules as in image (b and c).

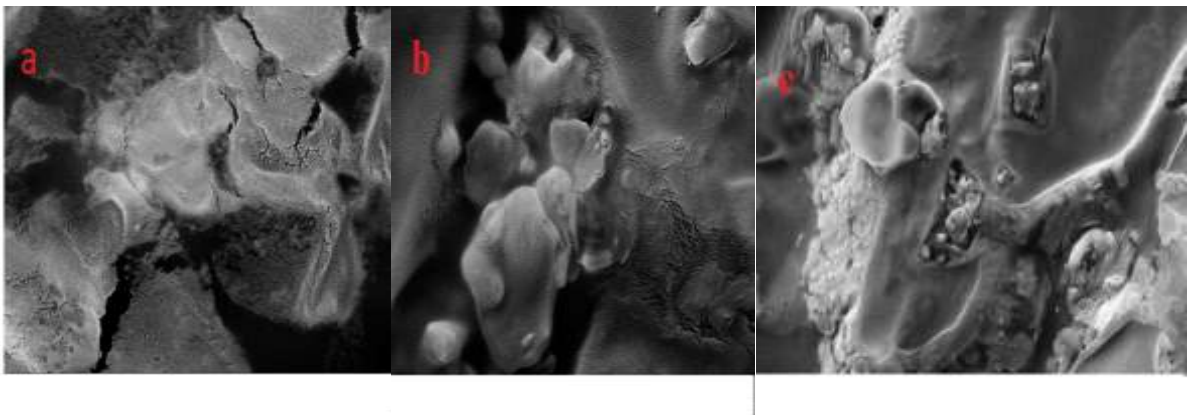

FIGURE 11 FESEM images of (V) compound

As for atomic force microscope (AFM) was also used to examine the morphology and the thickness of the compound (V) sheets. The morphology of this compound was pictured and measured using AFM in Figure 12.The maximum height of RGO-amide was 10.7 nm with the presence of gatherings on the surface. And that was supported by optional curve (240) nm from the measured sample at 500*500 nm.

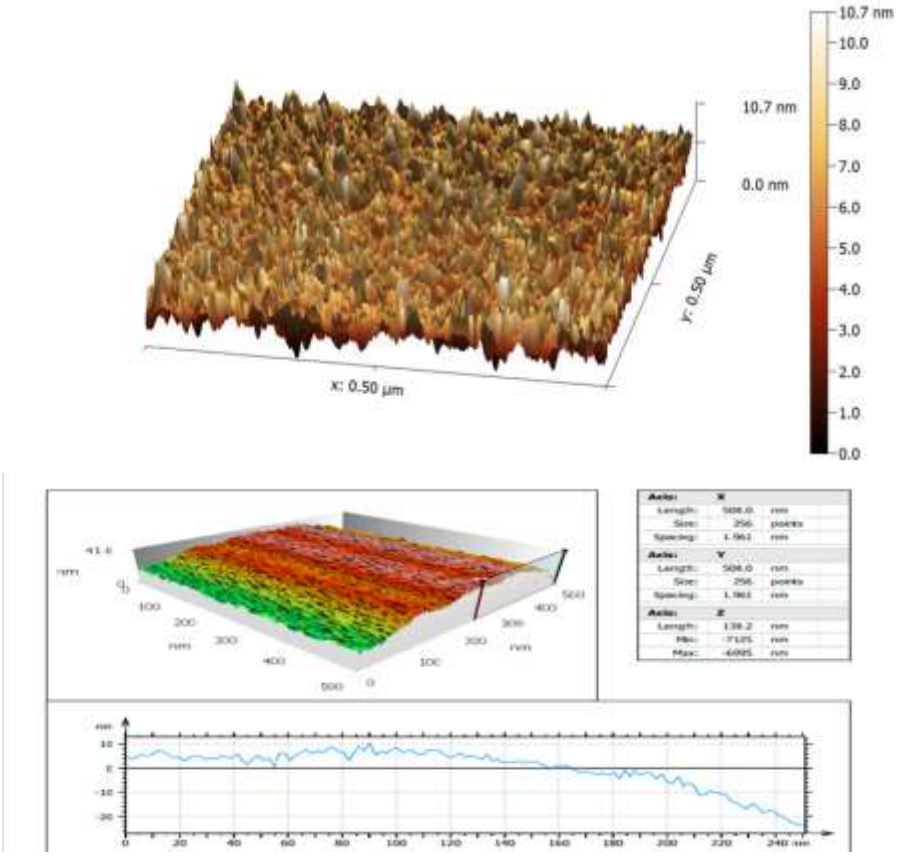

FIGURE 12 SEM Image of sample **SA_3** polymer nanocapsules

Biological analysis

The analysis revealed the cytotoxic effect of compound (V) that was tested at concentrations of [25 to 400 µM] on the viability of MCF-7 and WRL68 cells, after 24 hours of treatment. The results were recorded as mean and SD, as indicated in Table 1. The results showed a significant ability for compound (V) as anticancer activity on (MCF-7 and WRL68) cell lines at 50 µM.

TABLE 1 The MTT assay determined the IC50 values against MCF-7 and WRL-68 cells

Concentrations	MCF-7		WRL68	
µM	Mean	SD	Mean	SD
400.00	42.76	3.20	70.79	0.96
200.00	48.79	6.54	85.19	2.52
100.00	54.71	5.98	92.82	2.12
50.00	73.46	2.04	94.56	0.70
25.00	95.95	0.90	94.56	0.50

Data showed that the maximum dose responses (IC50) of WRL68 and MCF-7 at (272.2 and 32.97 µM) of (MCF-7 and WRL68), respectively, as depicted in Figure 13.The synthesized compound substantially improve the cytotoxicity against (MCF-7) and (WRL-68), and possessed the highest potency (the lowest IC50 values) with the lowest potency (the highest IC50 values); therefore, this compound is more selective for the type of breast cancer cell (MCF-7) and (WRL68 cells) that work as a vital strategy for treating drug resistant cancers in relation tothe commercial anticancer drugs.

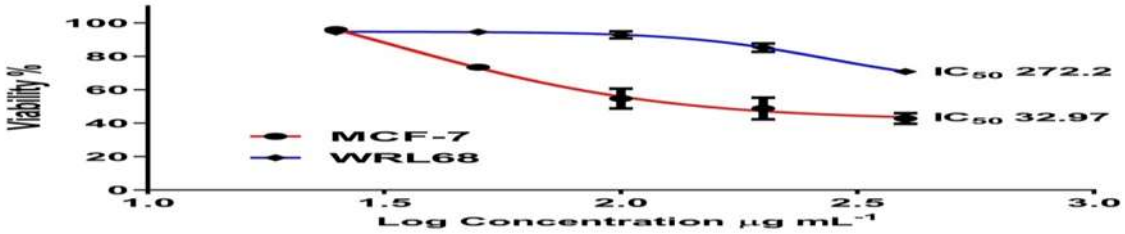

FIGURE 13 Dose-dependent cytotoxic effect of compound on MCF-7 and WRL-68 cells

Conclusion

The obtained data from the current study concluded that RGO-AMIDE compounds are more selective treatment for breast cancer cell (MCF-7) and (WRL68 cells) which could offer a new insights into the potential medical properties of compound and useful recommendations for the design of anti-tumor drugs in combating cancer owing to the existence of a broad variety of compounds which have therapeutic properties and improve the immune system.

Acknowledgements

We are thankful to Prof. Dr. Ghazwan Hasan Abdul Wahab (Department of Chemistry/ College of Education for pure Sciences/ Tikrit University/ Iraq) for explanation the xrd patterns, FESEM image, and AFM images for the new prepared compounds.

Orcid:

Hussein Ali Fadhil:
https://orcid.org/0000-0003-4864-2515
Ali H. Samir:
https://orcid.org/0000-0003-4664-7072
Yusra Abdulghafoor Mohammed:
https://orcid.org/0000-0003-4744-8171
Zeinab M.M. Al Rubae:
https://orcid.org/0000-0001-5263-154x

References

[1] S. Priyadarsini, S. Mohanty, S. Mukherjee, S. Basu, M. Mishra, *J. Nanostruct. Chem.*, **2018**, *8*, 123-137. [crossref], [Google Scholar], [Publisher]

[2] H. Sharma, S. Mondal, *Int. J. Mol. Sci.*, **2020**, *21*, 6280. [crossref], [Google Scholar], [Publisher]

[3] L. Liu, Q. Ma, J. Cao, Y. Gao, S. Han, Y. Liang, Y. Sun, *Cancer Nano.*, **2021**, *12*, 1-31. [crossref], [Google Scholar], [Publisher]

[4] S.C. Patel, S. Lee, G. Lalwani, C. Suhrland, S.M. Chowdhury, B. Sitharaman, *Ther. Deliv.*, **2016**, *7*, 101-116. [crossref], [Google Scholar], [Publisher]

[5] B. Datta, P.C. Adak, L.K. Shi, K. Watanabe, T. Taniguchi, J.C. Song, M.M. Deshmukh, *Science Advances*, **2019**, *5*, eaax6550. [crossref], [Google Scholar], [Publisher]

[6] Y. Li, W. Gao, L. Ci, C. Wang, P.M. Ajayan, *Carbon*, **2010**, *48*, 1124-1130. [crossref], [Google Scholar], [Publisher]

[7] S.K. Min, W.Y. Kim, Y. Cho, K.S. Kim, *Nature Nanotech.*, **2011**, *6*, 162-165. [crossref], [Google Scholar], [Publisher]

[8] H. Qian, B. Liu, X. Jiang, *Mater. Today Chem.*, **2018**, *7*, 53-64. [crossref], [Google Scholar], [Publisher]

[9] C.Y. Zhao, R. Cheng, Z. Yang, Z.M. Tian, *Molecules*, **2018**, *23*, 826. [crossref], [Google Scholar], [Publisher]

[10] P.N. Navya, A. Kaphle, S.P. Srinivas, S.K. Bhargava, V.M. Rotello, H.K. Daima, *Nano Convergence*, **2019**, *6*, 1-30. [crossref], [Google Scholar], [Publisher]

[11] M. Fiorillo, A.F. Verre, M. Iliut, M. Peiris-Pagés, B. Ozsvari, R. Gandara, M.P. Lisanti, *Oncotarget*, **2015**, *6*, 3553-3562. [crossref], [Google Scholar], [Publisher]

[12] J. Liu, H. Yang, S.G. Zhen, C.K. Poh, A. Chaurasia, J. Luo, X. Wu, E.K.L. Yeow, N.G. Sahoo, J. Lin, Z. Shen, *Rsc Adv.*, **2013**, *3*, 11745-11750. [crossref], [Google Scholar], [Publisher]

[13] K. Parvez, Z.-S. Wu, R. Li, X. Liu, R. Graf, X. Feng, K. Müllen, *J. Am. Chem. Soc.*, **2014**, *136*,

6083-6091. [crossref], [Google Scholar], [Publisher]
[14] P. Kumar, K. Subrahmanyam, C. Rao, *Int. J. Nanosci.,* **2011**, *10*, 559-566, [crossref], [Google Scholar], [Publisher]
[15] L. Shahriary, A.A. Athawale, *Int. J. Renew. Energy Environ. Eng.,* **2014**, *2*, 58-63. [Pdf], [Google Scholar], [Publisher]
[16] D.S. Chauhan, K. Ansari, A. Sorour, M. Quraishi, H. Lgaz, R. Salghi, *Int. J. Boil. Macromol.*, **2018**, *107*, 1747-1757. [crossref], [Google Scholar], [Publisher]
[17] M. Namvari, H. Namazi, *Polym. Int.,* **2014**, *63*, 1881-1888. [crossref], [Google Scholar], [Publisher]
[18] D.S. Chauhan, K.R. Ansari, A.A. Sorour, M. A. Quraishi, H. Lgaz, R. Salghi, *Int. J. Boil. Macromol.,* **2018**, *107*, 1747-1757. [crossref], [Google Scholar], [Publisher]
[19] N.H.N. Moorthy, U.B. Vittal, C. Karthikeyan, V. Thangapandian, A. Venkadachallam, P. Trivedi, *Arab. J. Chem*., **2017**, *10*, S3239-S3244. [crossref], [Google Scholar], [Publisher]
[20] A.H. Samir, R.S. Saeed, F.S. Matty, *Orient. J. Chem.*, **2018**, *34*, 286-294. [crossref], [Google Scholar], [Publisher]
[21] Y.A. Nagiev, *Russian J. Org. Chem.*, **2012**, *48*, 469-472. [crossref], [Google Scholar], [Publisher]
[22] K.S. Novoselov, A.K. Geim, S.V. Morozov, D. Jiang, Y. Zhang, S.V Dubonos, I.V. Grigorieva, A.A. Firsov, *Science,* **2004**, *306*, 666-669. [crossref], [Google Scholar], [Publisher]
[23] A.A.H. Sebeka, A.M. Osman, I.E.T. El Sayed, M. El Bahanasawy, M.A. Tantawy, *J. Appl. Pharm. Sci.*, **2017**, *7*, 9-15. [crossref], [Google Scholar], [Publisher]
[24] M. El-Far, G.A. Elmegeed, E.F. Eskander, H.M. Rady, M.A. Tantawy, *Eur. J. Med. Chem.*, **2009**, *44*, 3936-3946. [crossref], [Google Scholar], [Publisher]
[25] V.C. Abraham, D.L. Towne, J.F. Waring, U. Warrior, D.J. Burns, *J. Biomol. Screen.*, **2008**, *13*, 527-537. [crossref], [Google Scholar], [Publisher]
[26] K.S. Hmood, A.A.R.M. Kubba, *Syst. Rev. Pharm.*, **2021**, *12*, 1745-1762. [crossref], [Google Scholar], [Publisher]
[27] J. Zhou, D. Wu, D. Guo, *J. Chem. Technol. Biotechnol.*, **2010**, *85*, 1402-1406. [crossref], [Google Scholar], [Publisher]
[28] N.H.N. Moorthy, U.B. Vittal, C. Karthikeyan, V. Thangapandian, A.P. Venkadachallam, P. Trivedi, *Arab. J. Chem*., **2017**, *10*, S3239-S3244. [crossref], [Google Scholar], [Publisher]
[29] F.S. Matty, R.S. Saeed, A.H. Samir, *J. Glob. Pharma. Technol.*, **2017**, *10*, 345-355. [Pdf], [Google Scholar], [Publisher]
[30] A. Moretti, Q. Li, R. Chmielowski, L.B. Joseph, P.V. Moghe, K.E. Uhrich, *Nanomaterials*, **2018**, *8*, 84. [crossref], [Google Scholar], [Publisher]
[31] K.P. Barot, K.S. Manna, M.D. Ghate, *J. Saudi Chem. Soc.*, **2017**, *21*, S35-S43. [crossref], [Google Scholar], [Publisher]

How to cite this article: Hussein Ali Fadhil*, Ali H. Samir, Yusra Abdulghafoor Mohammed, Zeinab M.M. Al. Rubaei. Synthesis, Characterization and *in vitro* study of novelmodified reduced graphene oxide (RGO) containing heterocyclic compounds as anti-breast cancer. *Eurasian Chemical Communications*, 2022, 4(11), 1156-1170.
Link: http://www.echemcom.com/article_153130.html